Published in final edited form as:
J Immunol. 2012 December 15; 189(12): 5934–5941. doi:10.4049/jimmunol.1201851.

Role of Galectin-3 in Classical and Alternative Macrophage Activation in the Liver following Acetaminophen Intoxication[1]

Ana-Cristina Docan Dragomir[*], **Richard Sun**[*], **Hyejeong Choi**[*], **Jeffrey D. Laskin**[†], and **Debra L. Laskin**[*,2]

[*]Department of Pharmacology and Toxicology, Ernest Mario School of Pharmacy, Rutgers University, Piscataway, NJ 08854, USA

[†]Department of Environmental and Occupational Medicine, UMDNJ-Robert Wood Johnson Medical School, Piscataway, NJ 08854, USA

Abstract

Inflammatory macrophages have been implicated in hepatotoxicity induced by the analgesic, acetaminophen (APAP). In these studies we characterized the phenotype of macrophages accumulating in the liver following APAP intoxication and evaluated the role of galectin-3 (Gal-3) in macrophage activation. Administration of APAP (300 mg/kg, i.p.) to wild type mice resulted in the appearance of two distinct subpopulations of $CD11b^+$ cells in the liver, which expressed high or low levels of the monocyte/macrophage activation marker Ly6C. Whereas $CD11b^+/Ly6C^{hi}$ macrophages exhibited a classically activated proinflammatory phenotype characterized by increased expression of TNF-α, inducible nitric oxide synthase (iNOS), and CCR2, $CD11b^+/Ly6C^{lo}$ macrophages were alternatively activated, expressing high levels of the anti-inflammatory cytokine, IL-10. APAP intoxication was also associated with an accumulation of $Gal\text{-}3^+$ macrophages in the liver; the majority of these cells were $Ly6C^{hi}$. APAP-induced increases in $CD11b^+/Ly6C^{hi}$ macrophages were significantly reduced in $Gal\text{-}3^{-/-}$ mice. This was evident 72 h post-APAP and was correlated with reduced expression of the classical macrophage activation markers, iNOS, IL-12, and TNF-α, as well as the proinflammatory chemokines, CCL2 and CCL3, and chemokine receptors CCR1, and CCR2. Conversely, numbers of $CD11b^+/Ly6C^{lo}$ macrophages increased in livers of APAP-treated $Gal\text{-}3^{-/-}$ mice. This was associated with increased expression of the alternative macrophage activation markers Ym1 and Fizz1, increased liver repair and reduced hepatotoxicity. These data demonstrate that both classically and alternatively activated macrophages accumulate in the liver following APAP intoxication; moreover, Gal-3 plays a role in promoting a persistent proinflammatory macrophage phenotype.

Introduction

Liver injury caused by overdose of the analgesic acetaminophen (APAP) is the major cause of acute liver failure in the United States (1). APAP intoxication is characterized by centrilobular hepatocellular necrosis, which is initiated by covalent binding of the reactive APAP metabolite, N-acetyl-parabenzoquinoneimine (NAPQI), to critical protein targets in the liver (2). Evidence suggests that activated macrophages contribute to the pathogenic response to APAP. However, the role of these cells in APAP hepatotoxicity depends on their origin, the timing of their appearance in the liver, and the inflammatory mediators they encounter, which control their phenotype and function. Based on studies using macrophage

[1]This work was supported by NIH grants R01GM034310, R01ES004738, R01CA132624, U54AR055073 and P30ES005022.

[2]Corresponding author: Department of Pharmacology and Toxicology, Rutgers University, Ernest Mario School of Pharmacy, 160 Frelinghuysen Rd., Piscataway, NJ 08854, USA. Phone: 732-445-5862. Fax: 732-445-2534. laskin@eohsi.rutgers.edu.

inhibitors and transgenic mice, two subpopulations of macrophages have been identified in the liver after APAP intoxication that play distinct roles in hepatotoxicity: classically activated proinflammatory/cytotoxic macrophages, and alternatively activated anti-inflammatory/wound repair macrophages (3-7). It appears that the outcome of tissue injury depends on which macrophage subpopulation predominates. Thus, hepatotoxicity results from exaggerated or persistent responses of classically activated macrophages, whereas hepatoprotection is associated with increases in numbers of alternatively activated macrophages (reviewed in 8 and 9). The mechanisms regulating classical and alternative macrophage activation in the liver after APAP intoxication have not been established.

Gal-3 is a β-galactoside binding lectin secreted by macrophages in response to LPS, TNF-α, or IFN-γ (10, 11). Gal-3 acts in an autocrine and paracrine manner to promote macrophage release of proinflammatory mediators, including TNF-α, IL-12, CCL3, and CCL4, as well as reactive nitrogen species generated via inducible nitric oxide synthase (iNOS) (10-13). Loss of Gal-3 has been reported to result in reduced susceptibility to antigen-induced arthritis, renal ischemia-reperfusion injury, hypoxic-ischemic brain injury, and concanavalin A-induced hepatotoxicity, pathologies associated with exaggerated proinflammatory mediator activity (14-17). These findings led us to hypothesize that Gal-3 plays a role in promoting classical macrophage activation and inflammatory mediator production in the liver following APAP intoxication. This is supported by our findings of reduced hepatotoxicity and inflammatory mediator production in response to APAP in mice lacking Gal-3 (18). In the present studies, we extended these observations and characterized the role of Gal-3 in regulating the phenotype of hepatic macrophage subpopulations accumulating in the liver during APAP-induced hepatotoxicity. Results from these studies provide additional support for a contribution of Gal-3 to promoting inflammation in the liver following APAP intoxication.

Materials and Methods

Animals

Male specific pathogen-free C57Bl/6J wild type and Gal-3$^{-/-}$ mice (8-12 weeks old) were obtained from the Jackson Laboratory (Bar Harbor, ME). Gal-3$^{-/-}$ mice were backcrossed to a C57Bl/6 background for more than 10 generations. Mice were housed in microisolation cages and allowed free access to food and water. All animals received humane care in compliance with the institution's guidelines, as outlined in the *Guide for the Care and Use of Laboratory Animals*, published by the National Institutes of Health. Mice were fasted overnight prior to i.p administration of APAP (300 mg/kg) or PBS control. Mice were euthanized 24-72 h later with nembutal (200 mg/kg). Liver samples (100 mg aliquots) were collected and stored at −20°C in RNA*later* until RNA isolation. The remaining tissue was snap frozen in liquid nitrogen.

Hepatic nonparenchymal cell isolation

Nonparenchymal cells were isolated from the liver as previously described, with some modifications (19). The liver was perfused through the portal vein with warm Ca^{2+}/Mg^{2+}-free Hank's balanced salt solution (pH 7.3) containing 25 mM HEPES and 0.5 mM EGTA, followed by Leibowitz L-15 medium containing HEPES, 0.2 U/ml Liberase 3 Blendzyme, and 0.5 mg/ml protease type XIV. The liver was excised, disaggregated, and incubated with 2 mg/ml protease type XIV for 15 min at 37°C. The resulting cell suspension was filtered through a 220 μm nylon mesh. Hepatocytes were separated from nonparenchymal cells by four successive washes (50×g, 3 min). Supernatants containing nonparenchymal cells were centrifuged (300×g, 7 min), and the cells purified by density gradient centrifugation using

Optiprep medium (Sigma-Aldrich, St Louis, MO). Viability was assessed by trypan blue dye exclusion and was >95%.

Flow cytometry/cell sorting

Cells were analyzed immediately following isolation. Non-specific binding was blocked by incubation of the cells with anti-mouse-FcRII/III antibody (BD Biosciences, Franklin Lakes, NJ) for 5 min at 4°C. This was followed by 30 min incubation with FITC-conjugated anti-CD11b and PE-conjugated anti-Ly6C antibodies or isotype controls (BioLegend, San Diego, CA). Cells were then fixed in 3% paraformaldehyde, permeabilized in buffer containing 0.1% saponin, 0.1% sodium azide, and 1% fetal bovine serum in PBS, and stained with anti-Gal-3 antibody or goat IgG (R&D Systems, Minneapolis, MN), followed by isotype-specific AlexaFluor633-conjugated secondary antibody (Molecular Probes, Carlsbad, CA). Cells were analyzed using an FC500 flow cytometer (Beckman Coulter, Brea, CA). For sorting, cells were incubated with anti-mouse-FcRII/III antibody, followed by FITC-conjugated anti-CD45, AlexaFluor647-conjugated CD11b, and PE-conjugated anti-Ly6C antibodies (BioLegend, San Diego, CA) for 30 min. DAPI was added to the cell suspension immediately before analysis to exclude dead cells. Cells were sorted into $DAPI^{-}/CD45^{+}/CD11b^{+}/Ly6C^{hi}$ and $DAPI^{-}/CD45^{+}/CD11b^{+}/Ly6C^{lo}$ subpopulations using a Beckman Coulter MoFlo XDP Cell Sorter (Brea, CA), and immediately processed for RNA isolation.

Histology and immunohistochemistry

Livers were collected and 5 mm samples of the left lobes immediately fixed overnight at 4°C in 3% paraformaldehyde/2% sucrose. Tissue was washed three times in PBS containing 2% sucrose, and then transferred to 50% ethanol. After embedding in paraffin, 5 μm sections were prepared. For immunohistochemistry, sections were rehydrated and stained with antibody to PCNA (1:800, Abcam, Cambridge, MA), Ym1 (1:450, StemCell, Vancouver, BC) or IgG control (ProSci, Poway, CA). Binding was visualized using a Vectastain Elite ABC kit (Vector Laboratories, Burlingame, CA). Three to five random sections of each liver were examined.

Immunofluorescence

Liver samples (5 mm) were snap frozen in liquid nitrogen-cooled isopentane and embedded in OCT medium (Sakura Finetek, Torrance, CA). Six μm sections were prepared and fixed in 90% acetone/10% methanol. For double immunofluorescence, a sequential staining procedure was used (20). Sections were stained with anti-Ly6C antibody (1:50, AbD Serotec, Kidlington, UK), followed by isotype-specific AlexaFluor488-conjugated secondary antibody (Molecular Probes, Carlsbad, CA). After blocking with 5% rat serum, sections were stained with FITC-conjugated anti-F4/80 antibody (1:50, AbD Serotec, Kidlington, UK), followed by anti-FITC AlexaFluor488-conjugated secondary antibody. Images were acquired using a Leica SP5 confocal microscope (Leica Microsystems, Wetzlar, Germany). Identical laser power, gain and offset settings were used for all analyses.

Western blotting

Liver samples (30 mg) were lysed in buffer containing 20 mM HEPES, 150 mM NaCl, 10% glycerol, 1% Triton X-100, 1.5 mM $MgCl_2$, 1 mM diethylene-triamine pentaaacetic acid (DTPA), 1 mM phenylmethylsulfonylfluoride, 10 mM sodium pyrophosphate, 50 mM sodium fluoride, 2 mM sodium orthovanadate, and protease inhibitor cocktail. Protein concentrations were measured using the Bradford Assay (Bio-Rad, Hercules, CA). Proteins were separated on Tris-glycine polyacrylamide gels (Bio-Rad, Hercules, CA) and transferred onto nitrocellulose membranes. Non-specific binding was blocked by incubation of the blots for 1 h at room temperature with buffer containing 5% non-fat milk, 10 mM

Tris-base, 200 mM sodium chloride, and 0.1% polysorbate 20. Membranes were then incubated overnight at 4°C with anti-Gal-3 (1:2000) or anti-actin (1:1000) primary antibodies, followed by incubation with isotype-specific HRP-conjugated secondary antibodies (1:10,000) for 1 h at room temperature. Binding was visualized using an ECL Plus chemiluminescence kit (GE Healthcare, Piscataway, NJ).

Real-time PCR

Total RNA was isolated from liver samples using an RNeasy Mini kit, and from sorted monocytes/macrophages using an RNeasy Micro kit (Qiagen, Valencia, CA). RNA purity and concentration were measured using a Nanodrop spectrophotometer (Thermo Fisher Scientific, Wilmington, DE). RNA was converted into cDNA using a High Capacity cDNA Reverse Transcription kit according to manufacturer's directions (Applied Biosystems, Foster City, CA). Standard curves were generated using serial dilutions from pooled randomly selected cDNA samples. Real-time PCR was performed using SYBR Green PCR Master Mix (Applied Biosystems) on a 7900HT thermocycler (Applied Biosystems). All PCR primer pairs were generated using Primer Express 2.0 (Applied Biosystems), and synthesized by Integrated DNA Technologies (Coralville, IA). For each sample, gene expression changes was normalized relative to 18s RNA. Data are expressed as fold change relative to control. Forward and reverse primer sequences were: TNF-α, AGGGATGAGAAGTTCCCAAATG and TGTGAGGGTCTGGGCCATA; iNOS, GGCAGCCTGTGAGACCTTTG and TGAAGCGTTTCGGGATCTG; IL-12, CCTGGAGCACTC CCCATTC and TGCGCTGGATTCGAACAA; CCL2, TTGAATGTGAAGTTGACCCGTAA and GCTTGAGGTTGTGGAAAAG; CCL3, TCTTCTCAGCGCCATATGGA and TCCGGCTGTAGGAGAAGCA; CCL4, AGGGTTCTCAGCACCAATGG and CCGGGAGGTGTAAGAGAAACAG; CX3CL1, GCACAGGATGCAGGGCTTAC and TGTCAGCCGCCTCAAAACT; CCR1, CTGAGGGCCCGAACTGTTAC and GGCTAGGGCCCAGGTGAT; CCR5, TGATAAGCTGCAAAAAGCTGAAGA and GTCAGAGATGGCCAGGTTGAG; CCR2, TCCACGGCATACTATCAACATCTC and GGCCCCTTCATCAAGCTCTT; CX3CR1, TCGGTCTGGTGGGAAATCTG and GGCTTCCGGCTGTTGGT; Gal-1, CGGACGCCAAGAGCTTTGT and TGAAGTGTAGGCACAGGTTGTTG; found in inflammatory zone-1 (Fizz-1), CAGCTGATGGTCCCAGTGAA and TTCCTTGACCTTATTCTCCACGAT; Ym1, TCTGGTGAAGGAAATGCGTAAA and GCAGCCTTGGAATGTCTTTCTC; 18sRNA, CGGCTACCACATCCAAGGAA and GCTGGAATTACCGCGGCT.

Statistical analysis

Experiments were repeated two to three times. Data were analyzed using the Student's *t* test or one-way ANOVA followed by Dunn's post hoc analysis. A p value of < 0.05 was considered statistically significant.

Results

Distinct macrophage subpopulations accumulate in the liver following APAP intoxication

In our initial series of studies we used techniques in flow cytometry/cell sorting to assess the phenotype of macrophages accumulating in the liver after APAP intoxication. CD11b is the alpha chain of the Mac-1 integrin expressed on myeloid cells (21). APAP administration resulted in a time-related increase in $CD11b^+$ cells in the liver (Fig. 1, panels A and D). This was evident within 24 h and persisted for at least 72 h after APAP. To characterize these cells, we analyzed their expression of Ly6C, a surface antigen present at high levels on proinflammatory monocytes/macrophages (22). In livers of both control and APAP-treated mice, two distinct subpopulations of $CD11b^+$ cells were identified based on their expression

of Ly6C. These consisted of $Ly6C^{lo}$ cells and $Ly6C^{hi}$ cells (Fig. 1, panel A). In wild type mice, the majority of $CD11b^{+}$ cells expressed low levels of Ly6C. Following APAP administration, time-related increases in both $Ly6C^{lo}$ and $Ly6C^{hi}$ subpopulations were observed. Time-related increases in cells expressing Ly6C were also observed in histological sections following APAP administration (Fig. 2). These cells were mainly noted in centrilobular regions of the liver and were distinct from $F4/80^{+}$ resident Kupffer cells. In contrast to $Ly6C^{+}$ cells, $F4/80^{+}$ macrophages decreased in areas surrounding the central veins following APAP administration, a response which persisted for 48 h; subsequently, they began to reappear.

To further characterize the $Ly6C^{lo}$ and $Ly6C^{hi}$ macrophage subpopulations responding to APAP, the cells were sorted and examined microscopically. Giemsa staining confirmed that both subpopulations consisted of mononuclear phagocytes (Fig. 3, upper panel). $Ly6C^{lo}$ cells were enlarged relative to $Ly6C^{hi}$ cells, and more irregularly shaped. $Ly6C^{lo}$ cells also contained highly vacuolated cytoplasm, and displayed an increased cytoplasmic:nuclear ratio. RT-PCR analysis of the sorted cells revealed that $Ly6C^{hi}$ cells expressed higher mRNA levels of the proinflammatory proteins, TNF-α and iNOS, and the chemokine receptor CCR2, when compared to $Ly6C^{lo}$ cells (Fig. 3, lower panel). In contrast, mRNA expression of the anti-inflammatory cytokine IL-10 was reduced in $Ly6C^{hi}$ cells when compared to $Ly6C^{lo}$ cells.

Role of Gal-3 in macrophage activation in the liver following APAP intoxication

Consistent with our earlier studies (18), we found that APAP intoxication was associated with a time-dependent increase in Gal-3 protein expression in the liver, which was evident within 24 h and persisted for at least 72 h (Fig. 4, upper and middle panel). Immunostaining of the liver showed that Gal-3 was expressed by macrophages infiltrating into necrotic areas of the liver (Fig. 4, lower panel and 18). Flow cytometric analyses revealed that the majority of the $Gal\text{-}3^{+}$ macrophages infiltrating into the liver 24-48 h after APAP expressed high levels of Ly6C (Fig. 1, panel B). In contrast, in control mice, most Gal-3-positive macrophages were $Ly6C^{lo}$. APAP administration resulted in a decrease in the percentage of $Gal\text{-}3^{+}/LyC^{lo}$ cells at 24 h and 48 h; by 72 h, the percentage of these cells began to increase (Fig. 1, panel B).

We previously reported reduced injury and inflammation in the liver following APAP intoxication in mice lacking Gal-3 (18). In further studies we determined if this was associated with alterations in the macrophage subpopulations that appeared in the liver in response to APAP. Whereas loss of Gal-3 had no effect on the total number of $CD11b^{+}$ cells in the liver following APAP intoxication, a significant decrease in $CD11b^{+}/Ly6C^{hi}$ macrophages was observed (Fig. 1, panels C and D). This was associated with an increase in $CD11b^{+}/Ly6C^{lo}$ macrophages. Increased numbers of $CD11b^{+}/Ly6C^{lo}$ macrophages were also observed in PBS control-treated $Gal\text{-}3^{-/-}$ mice. Changes in liver macrophage subpopulations in APAP-treated $Gal\text{-}3^{-/-}$ mice were correlated with decreases in APAP-induced expression of the proinflammatory proteins IL-12, iNOS, and TNF-á, which was evident at 24 h and 48 h for IL-12, and at 48 h and 72 h for iNOS and TNF-á, as well as the chemokines CCL2 and CCL3, and the chemokine receptors CCR1 and CCR2, effects most prominent after 72 h (Figs. 5 and 6). Delayed CCL4 expression was also noted. Conversely, increases in expression of CX3CL1/CX3CR1 were observed in $Gal\text{-}3^{-/-}$ mice relative to wild type mice at 24 h post-APAP; however, by 72 h, CX3CR1 expression was reduced in these mice (Fig. 6). APAP-induced expression of CCR5 was not altered by loss of Gal-3 (Fig. 6). mRNA expression of Ym1 and Fizz-1, markers of alternatively activated anti-inflammatory/wound repair macrophages (23), was also increased in $Gal\text{-}3^{-/-}$ mice, when compared to wild type mice, after APAP administration (Figs. 5 and 7). Interestingly, whereas in control mice Ym1 protein was expressed in hepatic sinusoidal endothelial cells,

after APAP administration Ym1 was upregulated in macrophages (Fig. 7). This was first evident 48 h post-APAP, and was correlated with decreased Ym1 expression in endothelial cells. Loss of Gal-3 was associated with a more rapid and abundant increase in Ym1-positive macrophages in the liver, which was apparent within 24 h, and remained elevated for at least 72 h. In contrast, expression of the anti-inflammatory lectin, Gal-1, which increased in wild type mice 48 h and 72 h after APAP administration, was not significantly altered by loss of Gal-3 (Fig. 5). Alterations in liver macrophage subpopulations and inflammatory mediator expression in Gal-$3^{-/-}$ mice were also associated with increased repair of APAP-induced injury. Thus, significant increases in hepatocyte proliferation, as measured by the number of PCNA-positive cells and mitotic index, were observed in the livers of Gal-$3^{-/-}$ mice when compared to wild type mice (Figs. 8 and 9).

Discussion

Classically and alternatively activated macrophage subpopulations have been shown to play distinct roles in the pathogenesis of APAP-induced hepatotoxicity. Thus, while classically activated macrophages release cytotoxic/proinflammatory mediators which contribute to injury, alternatively activated macrophages down regulate inflammation and promote tissue repair (reviewed in 8). However, mechanisms regulating phenotypic activation of macrophages in the liver have not been established. The present studies demonstrate that Gal-3 plays a role in promoting persistent activation of proinflammatory/cytotoxic macrophages in the liver following APAP intoxication. These findings are important as they suggest a novel mechanism for classical macrophage activation during the pathogenesis of APAP-induced hepatotoxicity.

Evidence suggests that classically and alternatively activated macrophages accumulating in the liver after APAP-induced injury arise from distinct precursors (4-7,24). The present studies provide additional support for this concept. We confirmed that APAP intoxication results in a time related increase in $CD11b^+$ macrophages in the liver, which are distinct from resident Kupffer cells (6). Additionally, we demonstrated that these $CD11b^+$ cells are heterogeneous with respect to their expression levels of the macrophage activation marker, Ly6C. Thus two subpopulations were identified: cells expressing high levels of Ly6C and cells expressing low levels of Ly6C. Moreover, these $CD11b^+$ subpopulations are functionally distinct. Whereas $CD11b^+/Ly6C^{hi}$ macrophages exhibited a classically activated proinflammatory phenotype, characterized by increased mRNA expression of TNF-α, iNOS, and CCR2, $CD11b^+/Ly6C^{lo}$ macrophages expressed increased mRNA levels of the anti-inflammatory cytokine, IL-10, indicating that they are alternatively activated. Both $CD11b^+/Ly6C^{hi}$ and $CD11b^+/Ly6C^{lo}$ macrophage subpopulations were found to increase in number in the liver following APAP intoxication; the response of $Ly6C^{hi}$ macrophages was more robust than that of $Ly6C^{lo}$ macrophages. Accumulating $Ly6C^{hi}$ monocytes/macrophages have been reported to contribute to the development of tissue injury and inflammation in the liver induced by high-fat diet and carbon tetrachloride, as well as acute pancreatitis and myocardial infarction (25-28), and we speculate that they play a similar pathogenic role in APAP-induced hepatotoxicity.

APAP-induced increases in $CD11b^+/Ly6C^{lo}$ macrophages in the liver were also associated with the appearance of Ym1-positive alternatively activated macrophages in the tissue. Hepatic expression of the anti-inflammatory lectin, Gal-1, which is thought to promote alternative macrophage activation (29-31), also increased after APAP administration, suggesting a mechanism mediating their appearance in the liver. In contrast, APAP had no major effect on expression of Fizz-1, another marker of alternative macrophage activation (23). These data support the concept of subpopulation heterogeneity in alternatively activated macrophages (32). Depletion of alternatively activated macrophages with

clodronate liposomes is associated with a reduction in APAP-induced IL-10 expression in the liver and exaggerated hepatotoxicity (4). These data, along with reports that IL-10 plays a protective role in the liver following APAP intoxication (33,34), suggest that IL-10 producing $CD11b^{+}/Ly6C^{lo}$ cells are key to tissue repair in this model. This is supported by our findings that in Gal-$3^{-/-}$ mice, increases in $CD11b^{+}/Ly6C^{lo}$ cells were correlated with accelerated tissue repair, as measured by hepatocyte proliferation and reduced hepatotoxicity (18).

Following APAP intoxication we also observed a time related increase in Gal-3^{+} macrophages in the liver, which is in accord with our previous findings (18). The present studies show that these cells express high levels of Ly6C indicating a proinflammatory phenotype. Our observation that in the absence of Gal-3 the number of $Ly6C^{hi}$ macrophages appearing in the liver following APAP administration was significantly decreased, and that expression of the classical macrophage activation markers, iNOS, TNF-α and IL-12, and the proinflammatory chemokines and chemokine receptors, CCL2, CCL3, CCR1 and CCR2, was reduced, are in accord with this idea. The fact that $CD11b^{+}/Ly6C^{lo}$ anti-inflammatory/wound repair macrophages increased in livers of APAP-treated Gal-$3^{-/-}$ mice, and that this was correlated with a more rapid appearance of Ym1-positive macrophages in the tissue, and a marked increase in Fizz-1 expression, suggest a shift in the balance of macrophage subpopulations leading to accelerated tissue repair. Analogous increases in alternatively activated macrophages and hepatoprotection have been described in Gal-$3^{-/-}$ mice treated with concanavalin A (17). Of note is our observation that in control mice Gal-3 is expressed at low levels by $CD11b^{+}/Ly6C^{lo}$ cells, supporting previous reports that some liver resident macrophage subpopulations express this protein (18,35). Expression of Gal-3 on resident Kupffer cells is consistent with findings that these cells are constitutively activated due to continuous exposure to lipopolysaccharide in the portal circulation (36).

We also noted more rapid increases in peak expression of CX3CR1 and its ligand CX3CL1 in the livers of Gal-$3^{-/-}$ mice treated with APAP. CX3CR1 is highly expressed on anti-inflammatory/wound repair monocytes and macrophages (22), while CX3CL1 is produced primarily by hepatocytes and stellate cells following liver injury (37,38). CX3CL1 and CX3CR1 have been shown to play a protective role in toxin A-induced enteritis and carbon tetrachloride-induced liver inflammation and fibrosis, effects thought to be due to the recruitment of alternatively activated anti-inflammatory macrophages to sites of infection/injury (37,39). It remains to be determined if the CX3CL1/CX3CR1 signaling pathway is involved in hepatic recruitment of anti-inflammatory/wound repair macrophages following APAP intoxication.

A question arises as to the mechanisms underlying the appearance of proinflammatory macrophages in the liver following APAP intoxication. Our findings that peak expression of key proinflammatory mediators including TNF-α and IL-12, and chemokines like CCL2 and CCL4, precede maximal increases in $Ly6C^{hi}$/Gal-3^{+} macrophages in the liver suggest that the proinflammatory hepatic microenvironment promotes the development of classically activated macrophages. However, at present we cannot exclude the possibility that macrophages are recruited to the liver in response to Gal-3 or other chemokines, or danger-associated molecular patterns, such as high mobility group box-1 (HMGB1), released from APAP-injured hepatocytes (40-42). It appears that once localized in the liver, Gal-3^{+} macrophages play a role in maintaining the proinflammatory/cytotoxic microenvironment. In this regard, Gal-3 has been shown to upregulate expression of TNF-α, iNOS, and IL-12 in primary microglia and human monocytes (11,13). Moreover, reduced susceptibility to injury induced by streptozotocin, concanavalin A, or antigen-induced arthritis in Gal-$3^{-/-}$ mice is associated with decreased expression of these inflammatory proteins (14,17,43).

In contrast to our findings, Gal-3 has previously been reported to induce alternative activation in cultured macrophages (44). Differences between these results and our findings may be due to analysis of bone marrow-derived macrophages activated *in vitro* with defined concentrations of cytokines versus freshly isolated liver macrophages from APAP-injured mice. This may be important as Gal-3 expression and its intracellular distribution have been shown to be altered when primary macrophages are cultured *in vitro* (45).

In summary, the present studies identify and characterize multiple macrophage subpopulations accumulating in the liver following APAP intoxication, and demonstrate a role for Gal-3 in promoting persistent classical macrophage activation which contributes to hepatotoxicity. A more detailed understanding of the mechanisms regulating the phenotype of activated macrophages during APAP-induced liver injury may lead to the development of novel approaches to mitigating toxicity caused by this widely utilized analgesic.

Abbreviations used in this paper

APAP	acetaminophen
Fizz-1	found in inflammatory zone-1
GSH	glutathione
iNOS	inducible nitric oxide synthase
PCNA	proliferating cell nuclear antigen

References

1. Lee WM. Acute liver failure. Semin. Respir. Crit. Care Med. 2012; 33:36–45. [PubMed: 22447259]
2. Nelson, SD.; Bruschi, SA. Mechanisms of acetaminophen-induced liver disease. In: Kaplowitz, N.; DeLeve, LD., editors. Drug-Induced Liver Disease. 2nd ed. Informa Healthcare; New York, NY: 2007. p. 353-388.
3. Laskin DL, Gardner CR, Price VF, Jollow DJ. Modulation of macrophage functioning abrogates the acute hepatotoxicity of acetaminophen. Hepatology. 1995; 21:1045–1050. [PubMed: 7705777]
4. Ju C, Reilly TP, Bourdi M, Radonovich MF, Brady JN, George JW, Pohl LR. Protective role of Kupffer cells in acetaminophen-induced hepatic injury in mice. Chem. Res. Toxicol. 2002; 15:1504–1513. [PubMed: 12482232]
5. Dambach DM, Watson LM, Gray KR, Durham SK, Laskin DL. Role of CCR2 in macrophage migration into the liver during acetaminophen-induced hepatotoxicity in the mouse. Hepatology. 2002; 35:1093–1103. [PubMed: 11981759]
6. Holt MP, Cheng L, Ju C. Identification and characterization of infiltrating macrophages in acetaminophen-induced liver injury. J. Leukoc. Biol. 2008; 84:1410–1421. [PubMed: 18713872]
7. Gardner CR, Hankey P, Mishin V, Francis M, Yu S, Laskin JD, Laskin DL. Regulation of alternative macrophage activation in the liver following acetaminophen intoxication by stem cell-derived tyrosine kinase. Toxicol. Appl. Pharmacol. 2012; 262:139–148. [PubMed: 22575169]
8. Laskin DL. Macrophages and inflammatory mediators in chemical toxicity: a battle of forces. Chem. Res. Toxicol. 2009; 22:1376–1385. [PubMed: 19645497]
9. Laskin DL, Sunil VR, Gardner CR, Laskin JD. Macrophages and tissue injury: agents of defense or destruction? Annu. Rev. Pharmacol. Toxicol. 2011; 51:267–288. [PubMed: 20887196]
10. Liu FT, Hsu DK, Zuberi RI, Kuwabara I, Chi EY, Henderson WR Jr. Expression and function of galectin-3, a beta-galactoside-binding lectin, in human monocytes and macrophages. Am. J. Pathol. 1995; 147:1016–1028. [PubMed: 7573347]
11. Nishi Y, Sano H, Kawashima T, Okada T, Kuroda T, Kikkawa K, Kawashima S, Tanabe M, Goto T, Matsuzawa Y, Matsumura R, Tomioka H, Liu FT, Shirai K. Role of galectin-3 in human pulmonary fibrosis. Allergol. Int. 2007; 56:57–65. [PubMed: 17259811]

12. Papaspyridonos M, McNeill E, de Bono JP, Smith A, Burnand KG, Channon KM, Greaves DR. Galectin-3 is an amplifier of inflammation in atherosclerotic plaque progression through macrophage activation and monocyte chemoattraction. Arterioscler. Thromb. Vasc. Biol. 2008; 28:433–440. [PubMed: 18096829]
13. Jeon SB, Yoon HJ, Chang CY, Koh HS, Jeon SH, Park EJ. Galectin-3 exerts cytokine-like regulatory actions through the JAK-STAT pathway. J. Immunol. 2010; 185:7037–7046. [PubMed: 20980634]
14. Forsman H, Islander U, Andreasson E, Andersson A, Onnheim K, Karlstrom A, Savman K, Magnusson M, Brown KL, Karlsson A. Galectin 3 aggravates joint inflammation and destruction in antigen-induced arthritis. Arthritis Rheum. 2011; 63:445–454. [PubMed: 21280000]
15. Fernandes Bertocchi AP, Campanhole G, Wang PH, Goncalves GM, Damiao MJ, Cenedeze MA, Beraldo FC, de Paula Antunes Teixeira V, Dos Reis MA, Mazzali M, Pacheco-Silva A, Camara NO. A Role for galectin-3 in renal tissue damage triggered by ischemia and reperfusion injury. Transpl. Int. 2008; 21:999–1007. [PubMed: 18657091]
16. Doverhag C, Hedtjarn M, Poirier F, Mallard C, Hagberg H, Karlsson A, Savman K. Galectin-3 contributes to neonatal hypoxic-ischemic brain injury. Neurobiol. Dis. 2010; 38:36–46. [PubMed: 20053377]
17. Volarevic V, Milovanovic M, Ljujic B, Pejnovic N, Arsenijevic N, Nilsson U, Leffler H, Lukic ML. Galectin-3 deficiency prevents concanavalin A-induced hepatitis in mice. Hepatology. 2012; 55:1954–1964. [PubMed: 22213244]
18. Dragomir AC, Sun R, Mishin V, Hall LB, Laskin JD, Laskin DL. Role of galectin-3 in acetaminophen-induced hepatotoxicity and inflammatory mediator production. Toxicol. Sci. 2012; 127:609–619. [PubMed: 22461450]
19. Chen LC, Gordon RE, Laskin JD, Laskin DL. Role of TLR-4 in liver macrophage and endothelial cell responsiveness during acute endotoxemia. Exp. Mol. Pathol. 2007; 83:311–326. [PubMed: 17996232]
20. Lloyd CM, Phillips AR, Cooper GJ, Dunbar PR. Three-colour fluorescence immunohistochemistry reveals the diversity of cells staining for macrophage markers in murine spleen and liver. J. Immunol. Methods. 2008; 334:70–81. [PubMed: 18367204]
21. Dziennis S, Van Etten RA, Pahl HL, Morris DL, Rothstein TL, Blosch CM, Perlmutter RM, Tenen DG. The CD11b promoter directs high-level expression of reporter genes in macrophages in transgenic mice. Blood. 1995; 85:319–329. [PubMed: 7811988]
22. Robbins CS, Swirski FK. The multiple roles of monocyte subsets in steady state and inflammation. Cell. Mol. Life Sci. 2010; 67:2685–2693. [PubMed: 20437077]
23. Raes G, De Baetselier P, Noel W, Beschin A, Brombacher F, Hassanzadeh Gh G. Differential expression of FIZZ1 and Ym1 in alternatively versus classically activated macrophages. J. Leukoc. Biol. 2002; 71:597–602. [PubMed: 11927645]
24. Si Y, Tsou CL, Croft K, Charo IF. CCR2 mediates hematopoietic stem and progenitor cell trafficking to sites of inflammation in mice. J. Clin. Invest. 2010; 120:1192–1203. [PubMed: 20234092]
25. Deng ZB, Liu Y, Liu C, Xiang X, Wang J, Cheng Z, Shah SV, Zhang S, Zhang L, Zhuang X, Michalek S, Grizzle WE, Zhang HG. Immature myeloid cells induced by a high-fat diet contribute to liver inflammation. Hepatology. 2009; 50:1412–1420. [PubMed: 19708080]
26. Karlmark KR, Weiskirchen R, Zimmermann HW, Gassler N, Ginhoux F, Weber C, Merad M, Luedde T, Trautwein C, Tacke F. Hepatic recruitment of the inflammatory $Gr1^{+}$ monocyte subset upon liver injury promotes hepatic fibrosis. Hepatology. 2009; 50:261–274. [PubMed: 19554540]
27. Perides G, Weiss ER, Michael ES, Laukkarinen JM, Duffield JS, Steer ML. TNF-alpha-dependent regulation of acute pancreatitis severity by Ly-$6C^{(hi)}$ monocytes in mice. J. Biol. Chem. 2011; 286:13327–13335. [PubMed: 21343291]
28. Nahrendorf M, Swirski FK, Aikawa E, Stangenberg L, Wurdinger T, Figueiredo JL, Libby P, Weissleder R, Pittet MJ. The healing myocardium sequentially mobilizes two monocyte subsets with divergent and complementary functions. J. Exp. Med. 2007; 204:3037–3047. [PubMed: 18025128]

29. Correa SG, Sotomayor CE, Aoki MP, Maldonado CA, Rabinovich GA. Opposite effects of galectin-1 on alternative metabolic pathways of L-arginine in resident, inflammatory, and activated macrophages. Glycobiol. 2003; 13:119–128.
30. Cooper D, Iqbal AJ, Gittens BR, Cervone C, Perretti M. The effect of galectins on leukocyte trafficking in inflammation: sweet or sour? Ann. N. Y. Acad. Sci. 2012; 1253:181–192. [PubMed: 22256855]
31. Liu FT, Rabinovich GA. Galectins: regulators of acute and chronic inflammation. Ann. N. Y. Acad. Sci. 2010; 1183:158–182. [PubMed: 20146714]
32. Sica A, Mantovani A. Macrophage plasticity and polarization: in vivo veritas. J. Clin. Invest. 2012; 122:787–795. [PubMed: 22378047]
33. Bourdi M, Masubuchi Y, Reilly TP, Amouzadeh HR, Martin JL, George JW, Shah AG, Pohl LR. Protection against acetaminophen-induced liver injury and lethality by interleukin 10: role of inducible nitric oxide synthase. Hepatology. 2002; 35:289–298. [PubMed: 11826401]
34. Bourdi M, Eiras DP, Holt MP, Webster MR, Reilly TP, Welch KD, Pohl LR. Role of IL-6 in an IL-10 and IL-4 double knockout mouse model uniquely susceptible to acetaminophen-induced liver injury. Chem. Res. Toxicol. 2007; 20:208–216. [PubMed: 17305405]
35. Nibbering PH, Leijh PC, van Furth R. Quantitative immunocytochemical characterization of mononuclear phagocytes. II. Monocytes and tissue macrophages. Immunology. 1987; 62:171–176. [PubMed: 3315977]
36. Ahmad N, Chen LC, Gordon MA, Laskin JD, Laskin DL. Regulation of cyclooxygenase-2 by nitric oxide in activated hepatic macrophages during acute endotoxemia. J. Leukoc. Biol. 2002; 71:1005–1011. [PubMed: 12050186]
37. Aoyama T, Inokuchi S, Brenner DA, Seki E. CX3CL1-CX3CR1 interaction prevents carbon tetrachloride-induced liver inflammation and fibrosis in mice. Hepatology. 2010; 52:1390–1400. [PubMed: 20683935]
38. Karlmark KR, Zimmermann HW, Roderburg C, Gassler N, Wasmuth HE, Luedde T, Trautwein C, Tacke F. The fractalkine receptor CX(3)CR1 protects against liver fibrosis by controlling differentiation and survival of infiltrating hepatic monocytes. Hepatology. 2010; 52:1769–1782. [PubMed: 21038415]
39. Inui M, Ishida Y, Kimura A, Kuninaka Y, Mukaida N, Kondo T. Protective roles of CX3CR1-mediated signals in toxin A-induced enteritis through the induction of heme oxygenase-1 expression. J. Immunol. 2011; 186:423–431. [PubMed: 21131421]
40. Laskin DL, Pilaro AM, Ji S. Potential role of activated macrophages in acetaminophen hepatotoxicity. II. Mechanism of macrophage accumulation and activation. Toxicol. Appl. Pharmacol. 1986; 86:216–226. [PubMed: 3024357]
41. Sano H, Hsu DK, Yu L, Apgar JR, Kuwabara I, Yamanaka T, Hirashima M, Liu FT. Human galectin-3 is a novel chemoattractant for monocytes and macrophages. J. Immunol. 2000; 165:2156–2164. [PubMed: 10925302]
42. Dragomir AC, Laskin JD, Laskin DL. Macrophage activation by factors released from acetaminophen-injured hepatocytes: potential role of HMGB1. Toxicol. Appl. Pharmacol. 2011; 253:170–177. [PubMed: 21513726]
43. Mensah-Brown EP, Al Rabesi Z, Shahin A, Al Shamsi M, Arsenijevic N, Hsu DK, Liu FT, Lukic ML. Targeted disruption of the galectin-3 gene results in decreased susceptibility to multiple low dose streptozotocin-induced diabetes in mice. Clin. Immunol. 2009; 130:83–88. [PubMed: 18845486]
44. MacKinnon AC, Farnworth SL, Hodkinson PS, Henderson NC, Atkinson KM, Leffler H, Nilsson UJ, Haslett C, Forbes SJ, Sethi T. Regulation of alternative macrophage activation by galectin-3. J. Immunol. 2008; 180:2650–2658. [PubMed: 18250477]
45. Dumic J, Lauc G, Hadzija M, Flogel M. Transfer to in vitro conditions influences expression and intracellular distribution of galectin-3 in murine peritoneal macrophages. Z. Naturforsch. C. 2000; 55:261–266. [PubMed: 10817217]

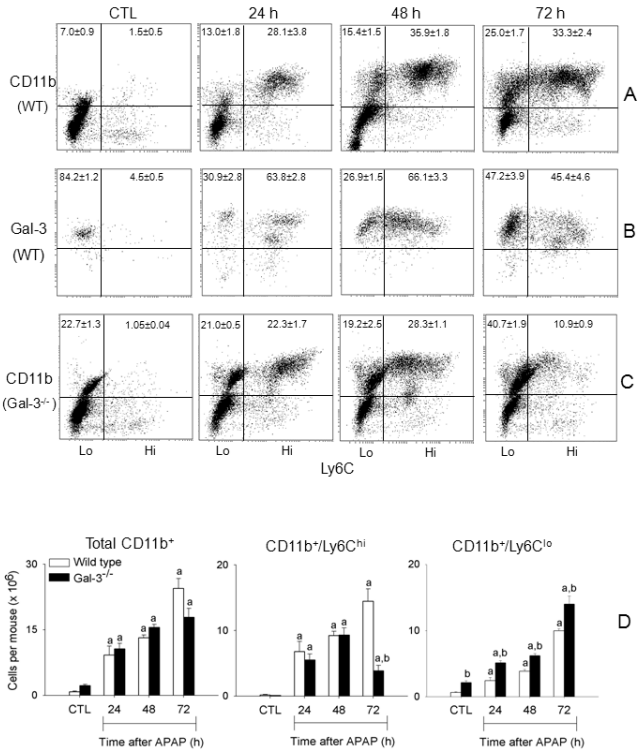

Fig. 1. Characterization of macrophage subpopulations in the liver following APAP intoxication

Liver nonparenchymal cells were isolated 24-72 h after treatment of wild type mice (panels A and B) or Gal-3$^{-/-}$ mice (panel C) with APAP or PBS control (CTL). Cells were stained with antibodies to CD11b, Ly6C and Gal-3, or appropriate isotypic controls as described in the Materials and Methods, and then analyzed by flow cytometry. *Panel A.* Expression of CD11b and Ly6C by liver nonparenchymal cells from wild type (WT) mice. *Panel B.* Expression of Ly6C and Gal-3 by CD11b^{+} nonparenchymal cells from WT mice. *Panel C.* Expression of CD11b and Ly6C by liver nonparenchymal cells from Gal-3$^{-/-}$ mice. The percentages (mean ± SE) of each cell population are indicated. One representative plot from 4-12 mice is shown. *Panel D.* The number of CD11b^{+} cells, CD11b^{+}/Ly6C^{hi} cells, and CD11b^{+}/Ly6C^{lo} cells was calculated from the percentage-positive cells relative to the total number of liver nonparenchymal cells recovered. Bars represent the mean ± SE (n=4-12 mice). [a]Significantly different ($p<0.05$) from CTL. [b]Significantly different ($p<0.05$) from wild type mice.

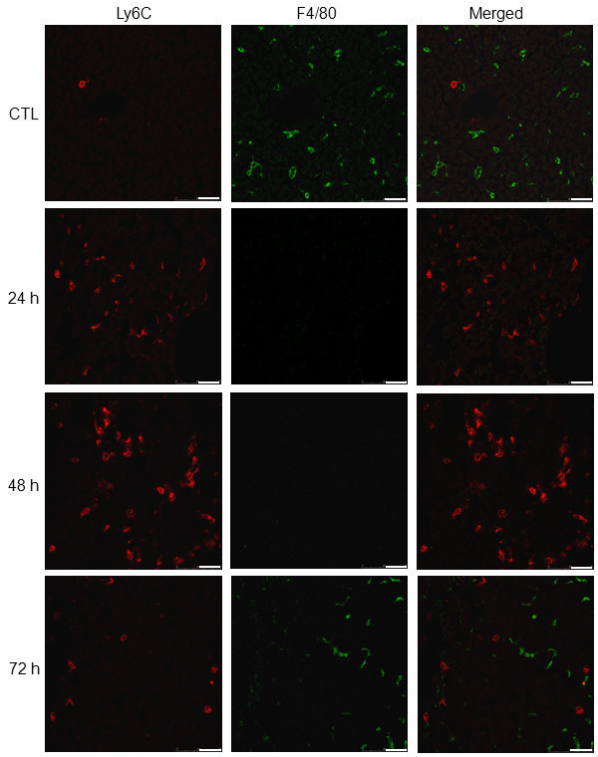

Fig. 2. Effects of APAP on liver macrophage expression of Ly6C and F4/80

Liver sections, prepared 24-72 h after treatment of wild type mice with APAP or PBS control (CTL), were sequentially stained with anti-Ly6C and anti-F4/80 antibodies, as described in the Materials and Methods. Scale bar, 25 μm. One representative section from 3-4 mice is shown.

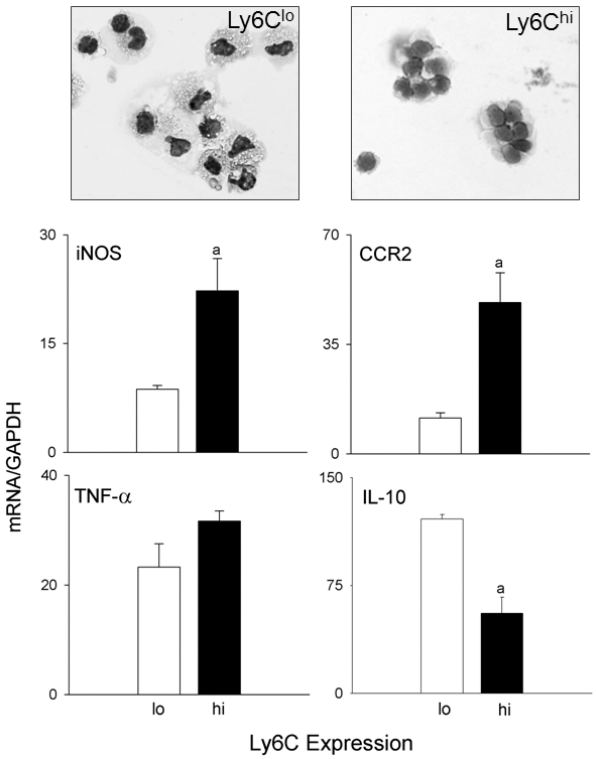

Fig. 3. Characterization of Ly6C^{hi} and Ly6C^{lo} macrophages accumulating in the liver following APAP intoxication

Liver nonparenchymal cells, isolated 48 h after treatment of wild type mice with APAP, were stained with anti-CD11b and anti-Ly6C antibodies, as described in the Materials and Methods. CD11b^{+} cells were sorted based on expression of Ly6C into CD11b^{+}/Ly6C^{hi} and CD11b^{+}/Ly6C^{lo} subpopulations. *Upper panel.* Cytospin preparations of sorted cells were stained with Giemsa. *Lower panel.* mRNA expression of sorted cells was assessed by RT-PCR. Data were normalized relative to GAPDH; bars represent mean ± SE (n=4-6).

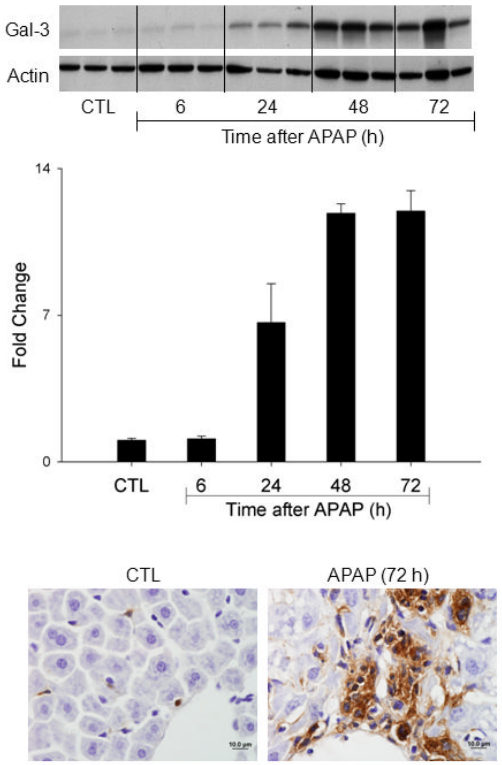

Fig. 4. Effects of APAP intoxication on Gal-3 expression in the liver

Livers were collected 6-72 h after treatment of wild type mice with APAP or PBS control (CTL). *Upper panel.* Gal-3 expression was analyzed by western blotting. Actin was used as the loading control. Each lane represents a different animal. *Middle panel.* Densitometric analysis was performed using ImageJ. Each bar represents the mean ± SE (n = 3 mice). *Lower panel.* Livers were collected 72 h after treatment of wild type mice with APAP or control. Gal-3 expression was analyzed by immunohistochemistry. One representative section from 6 mice is shown. Original magnification, 100x.

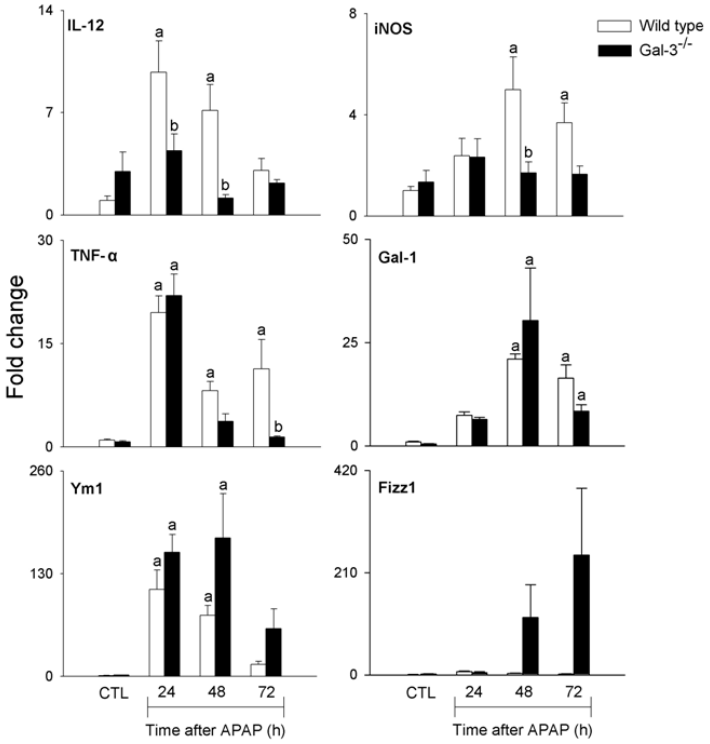

Fig. 5. Effects of APAP intoxication on expression of markers of classical and alternative macrophage activation

mRNA was prepared from liver samples 24-72 h after treatment of wild type and Gal-3$^{-/-}$ mice with APAP or PBS control (CTL), and analyzed by RT-PCR. Data were normalized to 18s RNA and presented as fold change relative to control. Each bar represents the mean ± SE (n=3-8 mice). [a]Significantly different ($p<0.05$) from CTL. [b]Significantly different ($p<0.05$) from wild type mice.

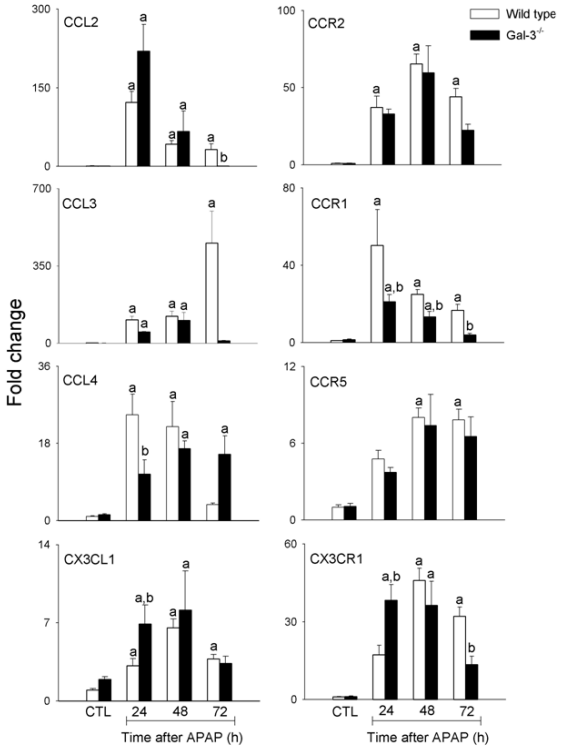

Fig. 6. Effects of APAP intoxication on expression of chemokines and chemokine receptors

mRNA was prepared from liver samples collected 24-72 h after treatment of wild type and Gal-$3^{-/-}$ mice with APAP or PBS control (CTL), and analyzed by RT-PCR. Data were normalized to 18s RNA and presented as fold change relative to PBS control. Each bar represents the mean ± SE (n=3-8 mice). aSignificantly different ($p<0.05$) from CTL. [b]Significantly different ($p<0.05$) from wild type mice.

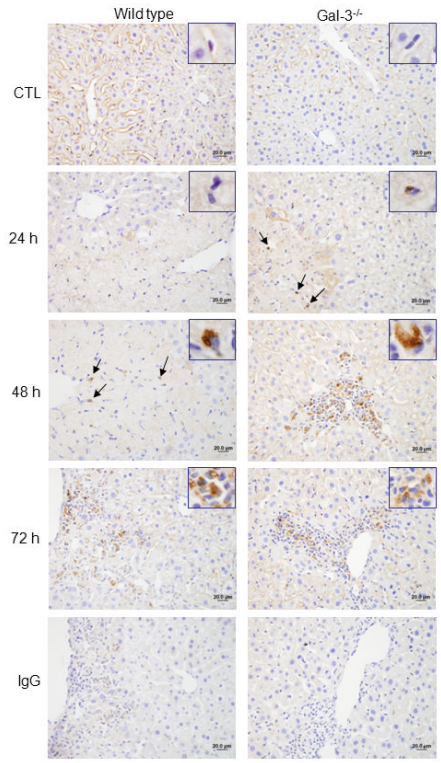

Fig. 7. Effects of APAP intoxication on Ym1 expression

Liver sections, prepared 24-72 h after treatment of wild type and Gal-3$^{-/-}$ mice with APAP or PBS control (CTL), were stained with anti-Ym1 antibody or IgG control. Binding was visualized using a Vectastain Elite ABC kit, with 3,3′-diaminobenzidine as substrate. One representative section from 3 mice is shown. Original magnification, 40x. Insets, 100x.

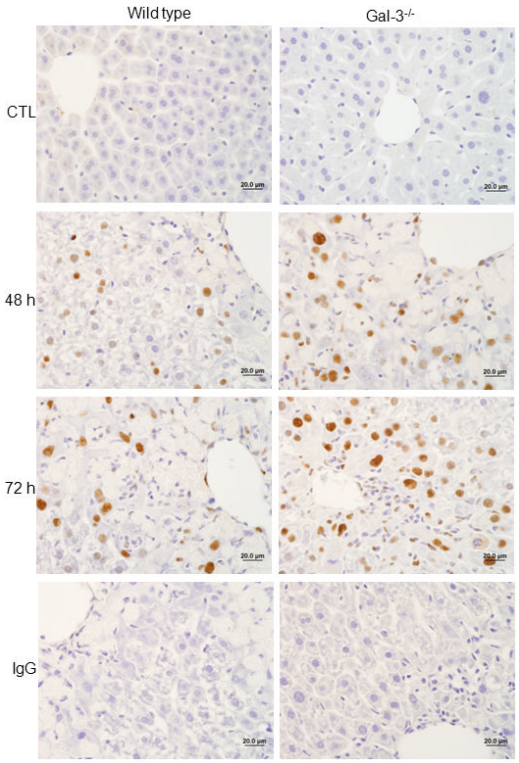

Fig. 8. Effects of APAP administration on PCNA expression

Liver sections, prepared 48-72 h after treatment of wild type and Gal-3$^{-/-}$ mice with APAP or PBS control, were stained with anti-PCNA antibody or IgG control. One representative section from 4-6 mice is shown. Original magnification, 63x.

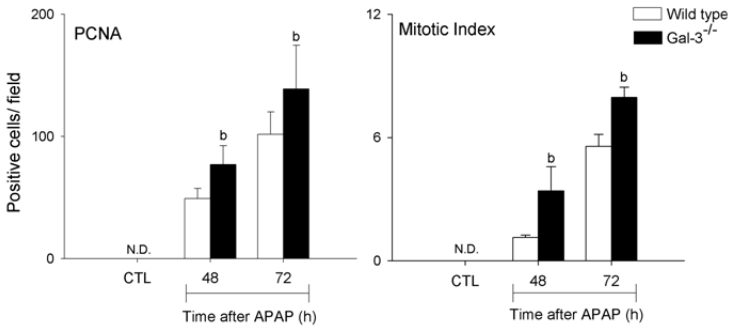

Fig. 9. Effects of loss of Gal-3 on liver repair following APAP intoxication

Liver sections were prepared 48-72 h after treatment of wild type and Gal-3$^{-/-}$ mice with APAP or PBS control (CTL). *Left panel.* Sections were stained with anti-PCNA antibody or IgG control. PCNA-positive hepatocyte nuclei were counted in six random fields per section (magnification 200x). Bars represent the mean ± SE (n=3-6 mice). [b]Significantly different ($p<0.05$) from wild type mice. *Right panel.* Sections were stained with hematoxylin and eosin and hepatocytes containing mitotic figure enumerated in 10-12 random fields. Mitotic index was calculated as the number of positive cells/field.